

A practical coherency model for spatially varying ground motions

Qing-Shan Yang[†] and Ying-Jun Chen[‡]

Department of Civil Engineering, Northern Jiaotong University, Beijing 100044, China

Abstract. Based on the discussion about some empirical coherency models resulted from earthquake-induced ground motion recordings at the SMART-1 array in Taiwan, and a heuristic model of the coherency function from elementary notions of stationary random process theory and a few simplifying assumptions regarding the propagation of seismic waves, a practical coherency model for spatially varying ground motions, which can be applied in aseismic analysis and design, is proposed, and the regressive coefficients are obtained using least-square fitting technique from the above recordings.

Key words: coherency function; practical model; strong ground motion; spatial variability.

1. Introduction

The time history of ground motion recorded by strong motion instruments has been traditionally focused in earthquake engineering, for instance, the response spectrum and the spectral density function in dynamic analysis and structural design. Meanwhile, it is noticed that the response of structures with large foundations or with widely spaced multiple supports will be influenced by the spatial as well as the temporal variation of ground motions (Iwan 1979).

The variability of the support motions usually tends to reduce the inertia-generated forces within the structure, but generate additional forces, known as pseudo-static forces. The resultants of the two sets of forces may exceed the level of forces generated in the structure with uniform support motions, particularly when the structure is stiff (Kiureghian and Neuenhofer 1992). So, the spatial variability of the ground motion has been being an interesting focus for earthquake engineering researchers.

The nature of the spatial variability of ground motions is well characterized by the coherency function, which can be defined for the ground acceleration processes at stations k and l in frequency domain as:

$$\rho_{kl}(f) = G_{kl}(f) / \sqrt{G_k(f)G_l(f)} \quad G_k(f)G_l(f) \neq 0 \quad (1)$$

where f denotes the frequency; $G_k(f)$ and $G_l(f)$ denote the auto-power spectral densities of the processes at stations k and l , respectively; and $G_{kl}(f)$ denotes the cross-power spectral density of the processes at these two stations.

In general, $\rho_{kl}(f)$ is a complex value and can be written in the form:

[†] Associate Professor

[‡] Professor

$$\rho_{kl}(f) = |\rho_{kl}(f)| \exp(i\theta_{kl}(f)) \quad (2)$$

in which the bounded modulus $|\rho_{kl}(f)|$, often called lagged coherency, is a measure of the linear statistical dependence between the two processes; and

$$\theta_{kl}(f) = \text{arctg} \left(\frac{\text{Im}(\rho_{kl}(f))}{\text{Re}(\rho_{kl}(f))} \right) \quad (3)$$

is the frequency dependent phase angle, where Im, Re refer to the imaginary and real parts of a complex function, and $i = \sqrt{-1}$.

Broadly speaking, the coherency function can be expressed based on the theory of stochastic wave propagation in random medium (Sobczyk 1985, Uscunski 1997 and Sato 1997). While, since the complexities involved in solving the theoretical equations seem to be appreciably beyond the present scope of our knowledge, especially for the application purposes, it was recommended to set up closely spaced seismography arrays which may supply the essential information for constructing empirical coherency function of seismic ground motions (Iwan 1979).

The first operated large-scale digital array is the SMART-1 (Strong Motion Array Taiwan) seismography array, and the availability of strong motion array data has motivated engineers and seismologists to study the coherency of earthquake excitations (Abrahamson 1991, Hao 1989, Harichandran *et al.* 1986, Harichandran 1991, Oliveira *et al.* 1991, Abrahamson *et al.* 1987, Zerva *et al.* 1997, Bolt *et al.* 1982) and quite a few empirical coherency models have been put forward (Abrahamson *et al.* 1991, Hao 1989, Harichandran 1991, Oliveira *et al.* 1991).

All these empirical models can show the varying tendency of the coherency function with its main influence factors such as the separate distance and the frequency. While, the functions of the empirical models seem to be selected arbitrarily, and the coefficients in these empirical models were determined for a certain earthquake event based on the array recordings. It is difficult for them to be applied directly in other practical sites. So, the application of them is now limited to verifying the built structures or theoretical analysis of structural responses using SMART-1 recordings of some certain earthquakes (Harichandran *et al.* 1996, Hao *et al.* 1995, Hao *et al.* 1996) and they have not been able to be extensively used in the practical engineering (Hu *et al.* 1994, Fan *et al.* 1992).

The difficulties of the theoretical models and that of the empirical models in practical application have drawn some researchers attention, and a heuristic model for coherency function was developed by Kiureghian (1996) based on some common ideas which are also expressed in Bolt *et al.* (1984), Abrahamson (1985), Darragh (1988), Hu (1996) preliminary, that the coherency function may be composed of incoherency effect, wave-passage effect and site-response effect. A further analysis will indicate that two parts of the coherency function, the lagged coherency and phase angle, are controlled by different factors respectively, i.e., the phase angle relates to the wave-passage effect and site-response effect, which are varying from one site to another, while the lagged coherency function depends on the incoherency effect, which can be considered to be statistically same for one site to another. So, the results about the phase angle obtained from SMART-1 seem not to be able to be extended to other engineering sites; and the statistic laws for lagged coherency function based on SMART-1 recordings can be recommended to other practical engineering sites.

As only the fundamental basic concepts were offered in the heuristic models, an explicit formula of the lagged coherency function with coefficients determine-needed is desired. Based on the basic rules and the boundary conditions, offered by Kiureghian (1996), and on the common tendency of the lagged coherency with its influence factors, a tentative explicit formula is put forward in this

paper, the coefficients in the formula are determined for each of the 17 earthquake events recorded by SMART-1. The results show that the defined explicit formula of the lagged coherency function is reasonably accurate.

It may be imagined, for the randomness of the passage medium, the values of the coherency function are different from one event to another, and the coherency for one site may not be the same as that of SMART-1 recordings. It is desirable to predict the coherency function of the future earthquake on a project site based on the SMART-1 recordings. So, a practical formula with reliability for predicting the coherency function on other sites is also established by means of visualizing the coherency of each array recording as a random sample and taking the average cooperation. The coefficients in this practical formula are obtained from 187 coherency function samples.

2. Studies on empirical models for coherency function

2.1. Two typical empirical models

Since SMART-1 was operated, a few empirical models have been developed (Abrahamson *et al.* 1991, Hao 1989, Harichandran 1991, Oliveira *et al.* 1991). From among them, the works of Harichandran (1986, 1991), Hao (1989) and Oliveira *et al.* (1991) are typical and representative. It is helpful to brief them.

2.1.1. Harichandran model

Harichandran (1986, 1991) considered the spatial and temporal correlation of each of the three components (two horizontal, i.e., epicentral (radical), normal-to-epicentral (tangential), components, and one vertical component) of the SMART-1 recordings, respectively, and, the following important conclusions were drawn:

1) For any one event, the coherency structure is different for the radical, tangential and vertical components. However, for all components the coherency tends to decay with increasing frequency and separation. Further investigation indicated that the magnitude of the coherency spectrum is approximately a function of the scalar separation and frequency, instead of much depending on the vector separation.

2) For a specified frequency the decay of the coherency is initially quite rapid, but tends to level off with increasing separation.

3) The coherency for the vertical component decays rapidly with separation, and for the separation greater than about 400m, the lagged coherency functions are of the order of 0.3 or less,

4) For some components, the decay of the lagged coherency with frequency displays a corner frequency effect, i.e., for frequencies less than a particular corner frequency the coherency functions are approximately constant, while they show significant decay at smaller frequencies.

The study leads to the following empirical coherency function:

$$\rho(f, d) = |\rho(f, d)| e^{i\varphi(f, d)} \quad (4)$$

where

$$|\rho(f, d)| = A \exp\left(-\frac{2d}{\alpha\theta(f)}(1-A+\alpha A)\right) + (1-A) \exp\left(-\frac{2d}{\theta(f)}(1-A+\alpha A)\right) \quad (5)$$

is the lagged coherency, $\theta(f)=k(1+(f/f_0)^b)^{-1/2}$, d is the separation distance and A , α , k , f_0 , b are five

Table 1 Parameters for Eq. (5) (Harichandran 1991)

Parameters		A	α	k	f_0	b	C_x
Event 20	radical	0.636	0.0186	31200	1.51	2.98	5200 m/s (N49°W)
	tangential	0.706	0.00263	257300	0.68	2.15	
Event 24	radical	0.481	0.0	∞	0.87	3.41	3500 m/s (N53° W)
	tangential	0.618	0.0173	50100	1.97	5.49	

parameters. The parameters were estimated for two far field events (its feature is shown in Table 2) recorded by SMART-1 through a comprehensive analysis (Harichandran 1991) and are specified in Table 1.

$$\varphi(f, d) = -2\pi f \frac{d \cdot C_x}{|C_x|^2} \quad (6)$$

is the phase angle and $d \cdot C_x$ denotes the dot product of separation distance and apparent velocity vector. Harichandran (1991) simplified the form of phase angle to be

$$\varphi(f, d) = -2\pi f \frac{d}{C_x} \quad (7)$$

2.1.2. Hao and Oliveira model

Hao (1989) and Oliveira (1991) took the vector of distance separation (shown in Fig. 1) account into their lagged coherence model for horizontal component:

$$\rho(f, d) = |\rho(f, d)| \exp(-ifd_L/C_x) \quad (8)$$

where

$$|\rho(f, d)| = \exp(-\beta_1 d_L - \beta_2 d_T) \exp((-\alpha_1 d_L^{1/2} - \alpha_2 d_T^{1/2})f^2) \quad d > 100m \quad (9)$$

$$\alpha_{1,2}(f) = \frac{a_{1,2}}{f} + b_{1,2}f + c_{1,2} \quad 0.05 \leq f \leq 10.0$$

$$\alpha_{1,2}(f < 0.05) = \alpha_{1,2}(f = 0.05) \quad \alpha_{1,2}(f > 10.0) = \alpha_{1,2}(f = 10.0) \quad (10)$$

and $\beta_1, \beta_2, a_1, b_1, c_1, a_2, b_2, c_2$ are regressive parameters.

Oliveira (1991) studied the data recorded in the inner ring of SMART-1 array for 17 events (the catalog of which are shown in Table 2), which, chosen from the collection of 51 recorded events (Abrahamson *et al.* 1987), were the ones recorded by more than 7 inner ring stations. The parameters in Eq. (9), obtained by least-square fitting technique, are presented in Table 3.

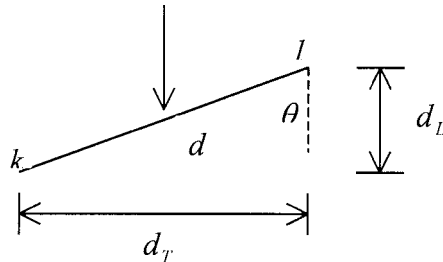


Fig. 1 Relative position of apparent velocity and stations

Table 2 Main features of earthquake event (Oliveira 1991)

Event No.		20	22	23	24	25	29	30	31	33	36	37	40	41	45	46	47	48
Magnitude		6.4	6.4	6.6	6.9	6.8	6.0	6.3	5.9	6.5	6.3	5.3	6.5	6.2	7.0			
Depth (Km)		87	28	37	44	28	9	61	4	3	6	2	16	22	7			
Distance (Km)		81	35	85	85	75	35	29	48	45	47	30	67	71	79	79	79	79
a_{\max} (gal)	V	31.8	36.7	12.4	15.4	11.0	23.5	34.9	36.8	38.2	55.4	41.0	72.5	28.5	110.3			
	EW	62.8	71.1	26.1	51.1	35.1	83.3	66.2	101.0	148.6	113.4	63.0	210.5	62.5	178.0			
	NS	86.1	64.0	36.1	64.9	38.5	65.0	78.7	69.2	97.2	82.8	73.4	251.1	99.8	251.0			

2.2. Comments on the empirical models

Some conclusions about the empirical models we may draw from some further studies are:

1) The conclusions drawn by Harichandran (Abrahamson *et al.* 1991, Hao 1989) are universal, i.e., they are suitable not only for the studied events but also for other events. While the parameters shown in Table 1, which are only for the radial and tangential two directions of the circular array, may be infeasible to extend them to the coherency of other stations with different relative directions.

2) Eqs. (6)-(8) indicate that the key to calculate the phase angle is how to determine the apparent velocity. Even though we have known there are preferential waves propagating from the epicentral area to the site and apparent velocities tend to increase with frequency increasing and to be noticeably smaller when frequencies are not greater than 2 Hz, it is believed (Hao 1989, Harichandran *et al.* 1986, Harichandran 1991) apparent velocity is the most difficult parameter to assess. This difficulty is due to the presence of the waves approaching from other directions with

Table 3 Parameters (Oliveira 1991)

Event No.	β_1	β_2	a_1	b_1	c_1	a_2	b_2	c_2
20	5.350 e-4	3.670 e-4	1.356 e-2	8.590 e-5	-1.933 e-3	4.554 e-3	1.697 e-3	-4.339 e-4
22	1.130 e-4	3.710 e-4	8.639 e-3	6.219 e-5	-1.251 e-3	2.644 e-3	-5.264 e-5	5.261 e-4
23	5.290 e-4	1.860 e-4	9.003 e-3	7.243 e-5	-1.445 e-3	7.016 e-3	2.420 e-5	-6.489 e-4
24	2.622 e-4	1.211 e-4	3.113 e-3	-6.635 e-6	2.042 e-5	3.286 e-3	2.590 e-6	-1.050 e-4
25	2.390 e-4	1.820 e-4	7.016 e-3	2.640 e-5	-6.749 e-4	1.583 e-2	1.903 e-4	-3.528 e-3
29	3.550 e-4	6.310 e-4	-4.177 e-4	-9.938 e-5	1.223 e-3	8.767 e-3	1.203 e-4	-2.007 e-3
30	2.250 e-4	5.100 e-4	1.066 e-2	2.651 e-5	-9.988 e-4	6.655 e-3	5.883 e-5	-1.118 e-3
31	4.620 e-4	4.820 e-4	7.483 e-3	7.660 e-5	-1.375 e-3	7.062 e-3	5.553 e-5	-1.168 e-3
33	2.810 e-4	3.710 e-4	3.624 e-3	-1.705 e-5	3.678 e-5	5.815 e-3	5.687 e-5	-1.005 e-3
36	3.530 e-4	2.830 e-4	8.240 e-4	1.267 e-5	-1.476 e-4	7.468 e-3	1.943 e-5	-6.911 e-4
37	7.910 e-4	6.830 e-4	1.186 e-2	1.451 e-4	-2.498 e-3	-1.124 e-2	-1.966 e-4	3.297 e-3
40	9.323 e-5	1.421 e-4	1.037 e-2	9.330 e-5	-1.821 e-3	8.090 e-3	4.083 e-5	-1.007 e-3
41	3.062 e-4	6.894 e-4	1.279 e-3	-9.656 e-6	1.225 e-4	4.355 e-3	4.282 e-5	-7.403 e-4
45	1.109 e-4	6.730 e-5	3.853 e-3	-1.811 e-5	1.177 e-4	5.163 e-3	-7.583 e-6	-1.905 e-4
46	1.193 e-3	9.010 e-4	2.025 e-3	1.802 e-5	-2.668 e-4	1.110 e-3	-4.701 e-5	5.659 e-4
47	7.420 e-4	1.202 e-3	1.883 e-3	5.172 e-6	-1.395 e-4	-1.872 e-3	-1.020 e-5	3.005 e-4
48	1.391 e-3	4.723 e-4	5.210 e-3	6.383 e-5	-1.036 e-3	-2.339 e-4	-6.473 e-5	9.687 e-4

Note: e-3 = $\times 10^{-3}$

diverse apparent velocities.

3) As it is shown there are some different opinions about the influence of the angle θ between the separation and the apparent velocity (Fig. 1) on the coherency, we give a further investigation on the coherency function in Hao and Oliveira model. Let the scalar distance d be fixed, and change the relative angle gradually, such as $d_T = (0.0, 0.1, \dots, 1.0)d$, $d_L = \sqrt{d^2 - d_T^2}$ and $\theta = \arctg(d_T/d_L)$, respectively, then compare their coherency functions. For example, the result for Event 45 as $d=300$ m is depicted in Fig. 2.

It is indicated that, from the practical application viewpoint, except the extreme cases, such as $d_T=0.0d$ and $d_T=1.0d$, the coherency is not too dependent on the vector separations. Actually, it is broadly believed that the coherency is more or less dependent on the angle θ , while the relationship between them is too complex to be determined reasonably and simply, it is acceptable to neglect its influence in the coherency function and consider its influence as the uncertainty.

4) In the same empirical model, the parameters vary remarkably from one event to another (Table 3), while it is found that the coherency curves for these events are fairly similar (as shown in Fig. 3, each curve is the average of 11 different directions shown in Fig. 2). This maybe indicate that these empirical models do not express the basic characteristics of the coherency function. The propagation of seismic wave should be considered more detail on the basis of some theoretical concepts.

3. Semi-empirical model for coherency function

3.1. Elementary principles of the theoretical model

As the shortcomings in the empirical models for the application purpose, a worthwhile heuristic model was developed by Kiureghian (1996), based on the common understandings and some fundamental theoretical concepts (Bolt *et al.* 1984, Abrahamson 1985, Abrahamson *et al.*, Darragh 1988, Hu 1996). Its main idea is that four distinct phenomena give rise to the spatial variability of earthquake-induced ground motions: (1) the loss of coherency of seismic wave due to scattering in the heterogeneous medium of the ground, as well as the differential superposition of waves arriving from an extended source, collectively denoted as the incoherence effect; (2) difference in the arrival times of waves at separate stations, denoted as the wave-passage effect; (3) gradual decay of wave amplitudes with distance due to geometric spreading and energy dissipation in the ground medium, denoted as the attenuation effect; (4) spatial variation of local soil profiles which influences the amplitude and frequency content of the bedrock motion underneath each station as it propagates upward, denoted as the site-response effect. As the attenuation effect is often insignificant for

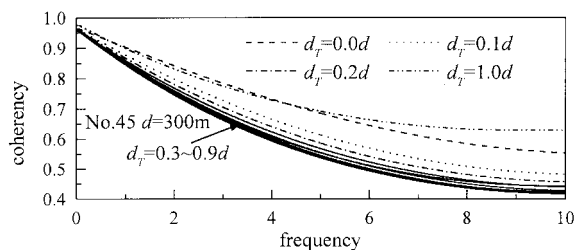


Fig. 2 Influence of separation vector on coherency

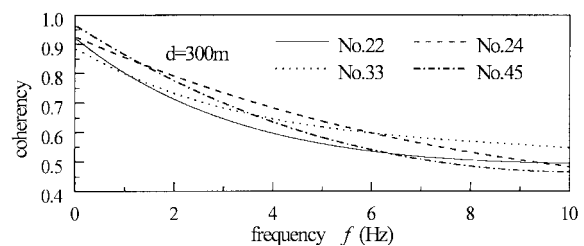


Fig. 3 Comparison of coherency for different events

typical size of man-made structures and has little influence on the coherency function, it can be ignored. So, the coherency function is:

$$\rho(f, d) = \rho(f, d)^{incoh} \cdot \rho(f, d)^{wave} \cdot \rho(f, d)^{site} \quad (11)$$

where $\rho(f, d)^{incoh}$, $\rho(f, d)^{wave}$, $\rho(f, d)^{site}$ denote the ‘incoherence’ effect, the ‘wave-passage’ effect and the ‘site-response’ effect, respectively.

Each term of Eq. (11) can be expressed in detail as:

$$\rho(f, d)^{site} = \exp\left(i\left(\arctg\frac{\text{Im}(H_k(f))}{\text{Re}(H_k(f))} - \arctg\frac{\text{Im}(H_l(f))}{\text{Re}(H_l(f))}\right)\right) \quad (12)$$

where $H_k(f)$, $H_l(f)$ denote the frequency response functions of the soil columns at stations k and l ;

$$\rho(f, d)^{wave} = \exp\left(i\left(-\frac{2\pi fd}{C_x}\right)\right) \quad (13)$$

$$\rho(f, d)^{incoh} = \cos(\beta(d, f))\exp(-0.5\alpha^2(d, f)) \quad (14)$$

and there are some boundary conditions that $\beta(d, f)$ and $\alpha(d, f)$ should satisfy

$$\lim_{d \rightarrow 0} \alpha(d, f) = \lim_{d \rightarrow 0} \beta(d, f) = 0 \quad (15.1)$$

$$\lim_{f \rightarrow 0} \alpha(d, f) = \lim_{f \rightarrow 0} \beta(d, f) = 0 \quad (15.2)$$

$$\lim_{d \rightarrow \infty} \alpha(d, f) = \lim_{f \rightarrow \infty} \alpha(d, f) = \infty \quad (15.3)$$

$$\lim_{d \rightarrow \infty} \beta(d, f) = \lim_{f \rightarrow \infty} \beta(d, f) = \frac{\pi}{2} \quad (15.4)$$

3.2. Function form of lagged coherency and parameter determining

What we should pay attention to the above model is that the ‘site-response’ effect and the ‘wave-passage’ effect control the phase angle spectrum. Further more, the ‘wave-passage’ effect is controlled by the apparent velocity, and it is known from the discussion in Sec.2 that the apparent velocity is also relevant to the site conditions. It may be inferred that the ‘wave-passage’ effect, as well as the ‘site-response’ effect, is determined by the local soil conditions, which means the phase angle is controlled by the local soil conditions. As the soil condition is different from one site to another, the statistic results about the phase angle obtained from SMART-1 recordings may not be able to be applied to other sites.

While, the incoherency effect only involves the lagged coherency function. As incoherency effect represents the scattering in the heterogeneous medium of the ground and the differential superposition of waves arriving from an extended source, it is controlled by the common randomness of the earthquakes and can be considered to have statistical regularity for different sites. So, the results for lagged coherency function obtained from SMART-1 array data may be able to be applied in other sites for the seismic response analysis and structural design.

For the purpose of seismic response analysis and structural design, an explicit form of $\beta(d, f)$ and $\alpha(d, f)$ corresponding to Eq. (14) is desired. It is apparent that the mapping forms, though they are not arbitrary, are not unique either. A wide variety of forms of $\beta(d, f)$ and $\alpha(d, f)$ may satisfy the

conditions of Eqs. (15). After a few times hard tests, it is believed that the following explicit functions for $\beta(d, f)$ and $\alpha(d, f)$ are rational and acceptable:

$$\beta(d, f) = \arctg(a_1 d^{0.25} + a_2 (df)^{0.5}) \quad (16)$$

$$\alpha(d, f) = a_3 a^4 f^{a_5} \quad (17)$$

So, the lagged coherency is:

$$\begin{aligned} |\rho(d, f)| &= \rho(d, f)^{incoh} \\ &= \cos(\arctg(a_1 d^{0.25} + a_2 (df)^{0.5})) \cdot \exp((-0.5(a_3 d^{a_4} f^{a_5})^2)) \\ &= (1 + (a_1 d^{0.25} + a_2 (df)^{0.5}))^{-0.5} \cdot \exp((-0.5(a_3 d^{a_4} f^{a_5})^2)) \end{aligned} \quad (18)$$

Using least-square fitting techniques, the parameter $a_1 \sim a_5$ in Eq. (18) are obtained for 17 events listed in Table 2 and they are presented in Table 4. The analysis accuracy is shown in Fig. 4. and Fig. 5.

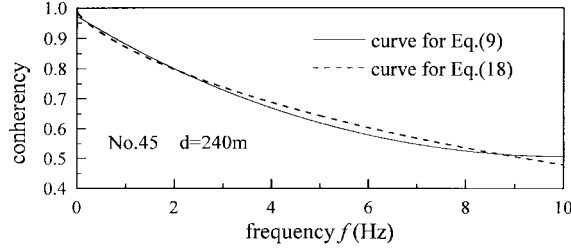
It can be seen from Table 4 that the scattering of the parameters for different events is quite similar to that of the coherency (Fig. 3). Fig. 4 shows that the analysis accuracy is satisfactory. Eq. (18) together with the coefficients in Table 4 becomes a semi-empirical coherency function based on the heuristic model of Kiureghian (1996).

4. The practical model for lagged coherency

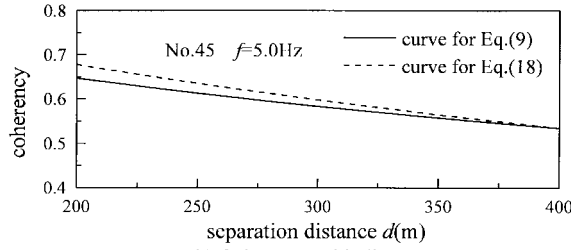
As shown above, the lagged coherency for different earthquake events and sites has similar varying tendency, and its magnitude on the same order, since it is controlled by the common

Table 4 Parameters for Eq. (18)

Event No.	a_1	a_2	a_3	a_4	a_5
20	0.150777E+00	0.112368E-01	0.467455E-01	0.438719E+00	0.205974E+00
22	0.707568E-01	0.698372E-03	0.726710E-01	0.377801E+00	0.287408E+00
23	0.144034E+00	0.694954E-02	0.466982E-01	0.431588E+00	0.235144E+00
24	0.876658E-01	0.134911E-01	0.344612E-01	0.325266E+00	0.580466E+00
25	0.936227E-01	-0.225546E-02	0.842473E-01	0.381519E+00	0.174161E+00
29	0.933706E-01	-0.176125E-02	0.814403E-01	0.368577E+00	0.199906E+00
30	0.912565E-01	-0.230008E-02	0.848887E-01	0.388581E+00	0.220384E+00
31	0.130032E+00	-0.363814E-02	0.784552E-01	0.385597E+00	0.150167E+00
33	0.957205E-01	-0.209288E-02	0.755358E-01	0.363117E+00	0.260197E+00
36	0.940179E-01	-0.171745E-02	0.742643E-01	0.355705E+00	0.228916E+00
37	0.146347E+00	0.612128E-02	0.611256E-01	0.362441E+00	0.238057E+00
40	0.431815E-01	-0.957183E-03	0.855492E-01	0.373131E+00	0.185215E+00
41	0.141102E+00	-0.491033E-02	0.538777E-01	0.389323E+00	0.287674E+00
45	0.376664E-01	-0.568746E-03	0.761072E-01	0.346510E+00	0.375780E+00
46	-0.361087E-02	0.227157E-01	0.715653E-01	0.437301E+00	-0.151703E-01
47	-0.659075E-01	0.144329E-01	0.680425E-01	0.440328E+00	0.147269E-01
48	-0.334315E-01	0.246126E-01	0.966675E-01	0.390934E+00	0.755371E-02

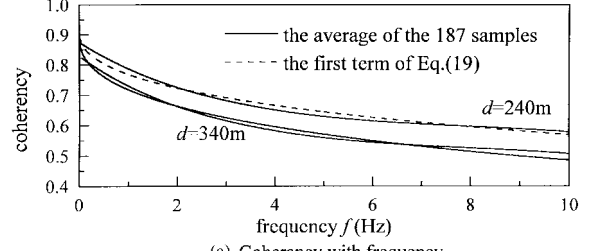


(a) Coherency with frequency

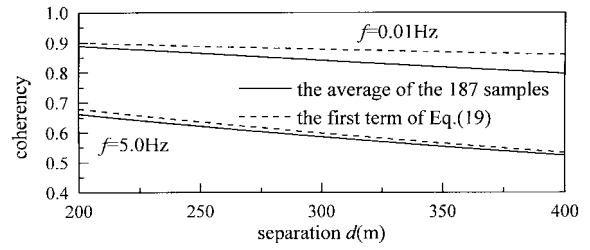


(b) Coherency with distance

Fig. 4 Lagged coherency for different models



(a) Coherency with frequency



(b) coherency with separation

Fig. 5 Simulation accuracy of the average lagged coherency

randomness. While, it is also within our expectation that the coherency for one event is different with one another, as indicated in Table 4. It is not reasonable to apply the lagged coherency of one event recorded by the SMART-1 array to predict that of an earthquake occurring on another engineering site. The authors believe that a simple but effective way perhaps is to take the array records as the random samples and determine the coherency function on average meaning using statistic method like determining the response spectrum:

$$S(f) = \bar{S}(f) \pm \mu \sigma_s(f)$$

where $\bar{S}(f)$ is the average value of response spectrum of $S(f)$; $\sigma_s(f)$ denotes the variance of $S(f)$; μ denotes the peak factor relevant to the reliability. While, there are also some differences between the response spectrum and the coherency function, in that the structural response increases with the increasing of the response spectrum, consistently, and there is not this consistence between the structural response and coherency function (Kiureghian and Neuenhofer), i.e., in some cases, the structural response may decrease with the increasing of coherency. For the structural safety, therefore, the practical model of coherency function should be:

$$|\rho(d, f)| = |\bar{\rho}(d, f)| \pm \mu \sigma_\rho(d, f) \quad (19)$$

where $|\bar{\rho}(d, f)|$ is the average value of $|\rho(d, f)|$; $\sigma_\rho(d, f)$ denotes the variance of $|\rho(d, f)|$; μ denotes the peak factor related to the required reliability of structures; the sign before μ is positive if the structural response increases with the increasing of coherency function, otherwise it is negative.

Assuming the function form of $|\bar{\rho}(d_{kl}, \omega)|$ is the same as Eq. (18), parameters $a_1 \sim a_5$ are obtained from the 17 events listed in Table 2 (each event has 11 different directions as shown in Fig. 2 to consider the influence of angle (θ) between the apparent velocity and the separation distance (Fig. 1) as a random factor) using the least square fitting technique. So, the total number of the sample function is 187. The results are presented in Table 5, and Fig. 5 shows the accuracy of regressive

Table 5 Parameters in $|\bar{\rho}(d, f)|$

a_1	a_2	a_3	a_4	a_5
0.115144E+00	-0.224874E-02	0.762306E-01	0.378401E+00	0.220597E+00

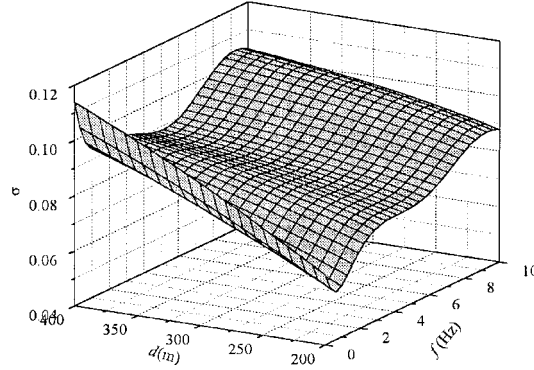


Fig. 6 Distribution of the sample variance

Table 6 Parameters in Eq. (20)

b_1	b_2	b_3	b_4	b_5	b_6
0.15132E+00	-0.87023E+00	0.10736E-03	-0.25960E-01	0.20221E-03	0.20716E+00

analysis.

The variance of these samples, σ_p , is displayed in Fig. 6. According to the varying tendency, like the determination of the form of Eqs. (16) and (17), the fitting function of the variance is selected as

$$\sigma_{pf}(d, f) = 0.2 \times \sin(b_1 f + b_2) + b_3 d + b_4 f + b_5 / (3 \times f) + b_6 \quad (20)$$

The values of parameters $b_1, b_2, b_3, b_4, b_5, b_6$ in Eq. (20) are presented in Table 6. The fitted variance σ_{pf} is depicted in Fig. 7. The error value, $\varepsilon = \sigma_{pf} - \sigma_p$, and its relative value $(\sigma_{pf} - \sigma_p) / \sigma_p$ are shown in Figs. 8 and 9. The relative error is about 10%.

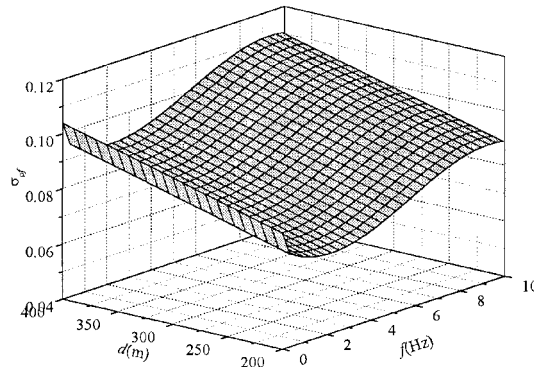


Fig. 7 Distribution of the fitted variance

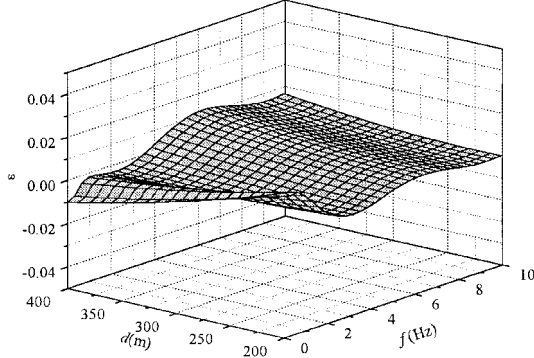


Fig. 8 The error of the fitted variance

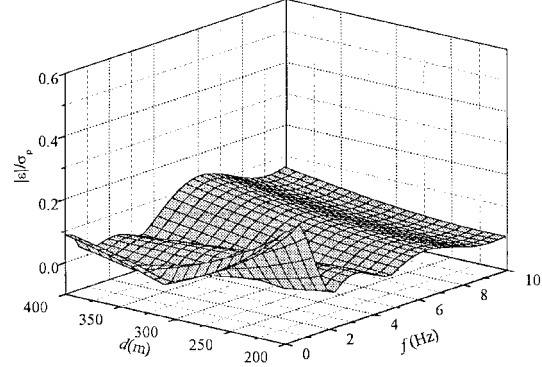


Fig. 9 The relative error of the fitted variance

5. Conclusions

In the heuristic coherency models for spatially varying ground motions, it is believed the spatial variability of earthquake ground motions is approximately determined by three distinct effects – incoherence effect, wave-passage effect and site-response effect. The incoherence effect is the loss of coherency of seismic wave due to scattering in the heterogeneous medium of the ground and the differential superposition of waves arriving from an extended source, which is related to the macroscopic uncertainty of the ground and epicenter while not much related to the local site conditions. So, It can be believed that incoherence effect is the same for one site as for another, and the statistical laws resulted from one site can be extended to another. Based on this idea, this paper, therefore, proposes a practical form for the incoherency effect, i.e., the lagged coherency:

$$\begin{aligned}
 |\rho(d, \omega)| &= |\bar{\rho}(d, \omega)| \pm \mu \sigma_\rho(d, \omega) \\
 &= (1 + (a_1 d^{0.25} + a_2 (df)^{0.5})^{-1/2} \cdot \exp((-\frac{1}{2}(a_3 d^{a_4} f^{a_5})^2) \\
 &\quad \pm \mu(0.2 \times \sin(b_1 f + b_2) + b_3 d + b_4 f + b_5 / (3.0 \times f) + b_6)
 \end{aligned} \tag{21}$$

The parameters in the above formula, $a_1 \sim a_5$ and $b_1 \sim b_6$, are determined and presented in Table 5 and 6. Should we obtain the parameters about the site conditions for an engineering field, combine Eq. (21) and Eqs. (12), (13), we can ascertain the coherency function for this field which can be applied in the practical seismic analysis and structural design.

In closing, it should be noted that any model may not be perfect, and the function developed in this paper is no exception. As mentioned above, the function form is not the only available one and the parameters maybe calibrated as the array data increase. Nevertheless the model developed in this paper may allow better calibration with specification of design motions for regions or geologic settings where no array recordings are available.

Acknowledgements

This study was supported by National Science Foundation of China. The support is gratefully acknowledged.

References

- Abrahamson, N.A. (1985), "Estimation of seismic wave coherency and rupture velocity using SMART-1 strong-motion array recordings", EERC Report No. UCB/EERC-85/12.
- Abrahamson, N.A. and Darragh, R.B., "Origin of scattered wave recorded by the SMART-1 strong motion array", *Seismic Research Letter*, **58**, 15.
- Abrahamson, N.A. Schneider, J.F. Stepp, J.C. (1991), "Empirical spatial coherency function for application to soil-structure interaction analysis", *Earthquake Spectra*, **7**, 1-28.
- Abrahamson, N.A., Bolt, B.A., Darragh, R.B., Penzien, J. and Tsai, Y.B. (1987), "The SMART-1 accelerometer array(1980-1987): A review", *Earthquake Spectra*, **3**, 267-287.
- Bolt, B. A. *et al.*, (1984), "The variation of strong ground motion over short distance", *8th WCEE*, San Francisco, **2**, 183-189; EERC Report No. UCB/EERC-84/13.
- Bolt, B.A., Loh, C.H., Penzien, J., Tsai, Y.B. and Yeh, Y.T. (1982), "Earthquake strong motions recorded by a large near-source array of digital seismographs", *Earthquake Engineering and Structural Dynamics*, **10**, 561-573.
- Darragh, R.B. (1988), "Analysis of near-source waves: Separation of wave types using strong motion array recordings", EERC Report No. UCB/EERC-88/08.
- Ding, H.P. and Liao, Z.P. (1996), "Assessment of phase spectrum of strong ground motion field for engineering purpose", *Earthquake Engineering & Engineering Vibration*, **16**(2), 76-86.
- Hao, H. (1989), "Multiple-station ground motion processing and simulation based on SMART-1 array data", *Nuclear Engineering and Design*, **111**, 293-310.
- Hao, H. and Duan, X.N. (1995), "Effect of multiple ground excitations on seismic response of asymmetric structures", *J. of Structural Engineering, ASCE*, **121**(11), 1557-1564.
- Hao, H. and Duan, X.N. (1996), "Multiple excitation effects on response of symmetric buildings", *Engineering Structures*, **18**(9), 732-740.
- Harichandran, R.S. (1991), "Estimation the spatial variation of earthquake ground motion from dense array recording", *Structural Safety*, **10**, 219-233.
- Harichandran, R.S. Vanmarke, E.H. (1986), "Stochastic variation of earthquake ground motion in space and time", *J. of Engineering Mechanics*, **112**(2), 154-174.
- Harichandran, R.S., Hawwari, A. and Sweden, B.N. (1996), "Response of long-span bridges to spatially varying ground motion", *J. of Structural Engineering*, **122**(5), 476-484.
- Hu, Y-X., Liu, S-C. and Dong, W. (1996), *Earthquake Engineering*, E & FN SPON.
- Iwan, W.D. (1979), "The development of strong-motion earthquake instrument arrays", *Earthquake Engineering and Structural Dynamics*, **7**, 413-426.
- Kiureghian, A. Der and Neuenhofer, A. (1992), "Response spectrum method for multiple-support seismic excitation", *Earthquake Engineering and Structural Dynamics*, **21**, 713-740.
- Kiureghian, A. Der. (1996), "A coherency model for spatially varying ground motions", *Earthquake Engineering and Structural Dynamics*, **25**, 99-111.
- Fan, Lichu, Yuan, Wangchen and Hu, Shide (1992), "The longitudinal seismic response analysis for Shanghai Nanpu Bridge", *China Civil Engineering Journal*, **25**(3), 2-8.
- Oliveira, C.S., Hao, H. Penzien, J. (1991), "Ground motion modeling for multiple-input structural analysis", *Structural Safety*, **10**, 79-93.
- Sato, Haruo (1997), *Seismic Wave Propagation and Scattering in the Heterogeneous Earth*, AIP Press.
- Hu, Shide and Fan, Lichu (1994), "The longitudinal earthquake response analysis for the Jiangyin Yangtze River Bridge", *J. of Tongji University*, **22**(1), 433-438.
- Sobczyk, K. (1985), *Stochastic Wave Propagation*, Elsevier, Boston.
- Uscunski, B.J. (1997), *The Elements of Wave Propagation in Random Media*, McGraw-Hill, New York.
- Zerva, A. and Zhang, O. (1997), "Correlation patterns in characteristics of spatially variable seismic ground motions", *Earthquake Engineering and Structural Dynamics*, **26**, 19-39.